



Grafting effect on the wetting and electrochemical performance of carbon cloth electrode and polypropylene separator in electric double layer capacitor

Izabela Stepniak*, Aleksander Ciszewski

Poznan University of Technology, Institute of Chemistry and Technical Electrochemistry, ul. Piotrowo 3, 60-965 Poznan, Poland

ARTICLE INFO

Article history:

Received 25 November 2009

Received in revised form 8 February 2010

Accepted 13 February 2010

Available online 20 February 2010

Keywords:

Electrochemical capacitor

Plasma-induced grafting

Acrylic acid

Lithium hydroxide

ABSTRACT

Activated carbon (AC) fiber cloths and hydrophobic microporous polypropylene (PP) membrane, both modified by plasma-induced graft polymerization of acrylic acid (AAc) under UV irradiation, and filled with saturated lithium hydroxide solution were used as electrodes, a separator and electrolyte in electric double layer capacitors (EDLCs). The modification process changed the hydrophobic character of AC and PP materials to hydrophilic, made them wettable and serviceable as components of an electrochemical capacitor. The presence of poly(acrylic acid) on the AC and PP surface was confirmed by SEM and XPS methods. Electrochemical characteristics of EDLCs were investigated by cyclic voltammetry and galvanostatic charge–discharge cycle tests and also by impedance spectroscopy. At the 1000th cycle of potential cycling (1 A g^{-1}) the specific capacitance of 110 F g^{-1} was obtained with a specific energy of 11 Wh kg^{-1} at power density of 1 kW kg^{-1} . The above results provide valuable information which may be used when developing novel compositions of EDLCs.

© 2010 Elsevier B.V. All rights reserved.

1. Introduction

The importance of energy storage devices has been constantly growing with the recently increasing popularity of various portable electronic devices and motor vehicles. One type of such energy storage devices are electric double layer capacitors (EDLCs), relatively new electrochemical energy storage media with a somewhat lower specific energy, but much higher specific power and longer cycle life than most rechargeable batteries. EDLCs are now under urgent scrutiny for extensive possible uses in power electronics for back-up memories and peak power saving [1–3]. While the storage of electric charges in batteries is based on reversible Faradic electrode reactions, in capacitors it occurs in the electric double layer at the electrode/electrolyte interface. Therefore, various types of polarizable electrodes based on activated carbons have been developed, i.e. paste type, activated carbon fiber cloth type, activated carbon fiber sheet type and activated carbon–carbon composite type, which exhibit a high specific surface area of the order of $10^3 \text{ m}^2 \text{ g}^{-1}$ [4]. However, specific capacitances obtained from carbon materials are usually much lower than expected. This is primarily attributed to poor wettability of the electrode material in an electrolyte solution, which results in a less accessible surface area for the formation of the electric double layer; it brings about high resistance to the transport of electrolyte ions within micropores of porous carbon

during charge/discharge processes. Therefore, it is mandatory for electrode material to exhibit good wettability to the electrolyte solution if good EDLC performance is expected. This explains why several treatments have been proposed to increase their specific capacitance, such as chemical surface oxidation in nitric acid solutions [5,6] or H_2SO_4 solution [7], activation by KOH [8,9] and NaOH [10], by polymer deposition [11,12] or by electrochemical modification [6,13]. To achieve high specific power and energy as well as a long cycle life, EDLC engineering is crucial.

Recently, the treatment with “cold plasma”, i.e. plasma generated at low temperature, has been used as a novel method for the modification of the physical and chemical properties of carbon materials. For example, the modification of activated carbon fiber cloth electrodes was performed by cold plasma in the Ar/O_2 atmosphere and the effect of its cold plasma treatment on the capacitor performance was discussed in terms of functional groups and pore size distributions of the electrode surface [14]. Furthermore, Li and Horita [15] mentioned that the carbon black surface was modified by low temperature oxygen plasma, it changed from hydrophobic to hydrophilic and the number of its functional groups containing oxygen increased. Cascarini De Torre et al. [16] stated that graphitized carbon black, after the oxygen-plasma treatment, changed its surface character from hydrophobic to hydrophilic. Moreover, Li and co-workers [17,18] showed the usefulness of radio frequency oxygen-plasma treatment for the modification of carbon materials and their use as electrode materials for EDLCs.

In this study we covalently attached polyacrylic acid (poly(AAc)) to the surfaces of activated carbon fiber cloth (AC) and the

* Corresponding author. Tel.: +48 616652317, fax: +48 616652571.

E-mail address: izabela.stepniak@put.poznan.pl (I. Stepniak).

hydrophobic polypropylene membrane (PP), using the plasma-induced grafting technique, to produce hydrophilic and readily wettable electrodes and separator materials by aqueous electrolytes. This modification is proposed to enhance the capacitance of AC electrodes. Finally, the performance of a double layer capacitor using these modified components and saturated lithium hydroxide as electrolyte is discussed.

2. Experimental

2.1. Materials

In this study a microporous PP membrane (Celgard 2500, Daicel Chemical Industries Ltd.; pore size of $0.05 \mu\text{m} \times 0.20 \mu\text{m}$, thickness of $25.4 \mu\text{m}$ and porosity of 45%) and an activated carbon (AC) fiber cloths (Kynol® Europa GmbH, No ACC with a specific surface area of ca. $2000 \text{ m}^2 \text{ g}^{-1}$) were used for the experimental EDLCs as separator and electrode materials. Acrylic acid (AAc) (Aldrich Chem. Co., Ltd.) was vacuum distilled prior to use. Acetic acid and lithium hydroxide were supplied by POCh, Gliwice, Poland, and argon by Linde Gas, Poland. Redistilled water was used in all experiments.

2.2. Plasma reactor

A microwave plasma generator with a frequency of 2.45 GHz and power ranging from 0 to 1000 W (Ertec, Wroclaw, Poland) was used throughout this study. Plasma was generated in a quartz tube at the top of a thick-walled glass reaction chamber of 80 mm in length and 100 mm in diameter. The PP membrane (or AC) was attached to the table in the post-discharge area; the distance of the sample to the lower edge of plasma could be regulated. Before plasma treatment, the reactor was evacuated to a pressure below 10^{-3} mbar. Gas flow was adjusted to the desired value and plasma at the desired power level was ignited for a predetermined time.

2.3. Grafting procedure

Samples of PP or AC ($4.0 \text{ cm} \times 4.0 \text{ cm}$) were placed into the plasma reactor and treated with argon plasma at desired parameters (plasma parameters: $V_{\text{Ar}} = 15 \text{ cm}^3 \text{ min}^{-1}$, power = 100 W, time 1–10 min (AC1 2.5, AC2 5.0, AC3 7.5, AC4 10 min), sample-to-plasma distance = 30 mm). Both sides of the objects were modified in the same way. After being taken out from the reactor, the sample was allowed to stay for 10 min in air atmosphere and then immersed in a de-aerated aqueous solution of acrylic acid (water:acetic acid:AAc = 1:1:0.5) and exposed to a wide-range UV radiation for the desired time (AC1 2.5, AC2 5.0, AC3 7.5, AC4 10 min); details of this procedure was presented previously [19,20]. To remove poly(acrylic acid) not covalently bound to the surface of modified materials, samples were washed extensively in water and next immersed in saturated aqueous lithium hydroxide solution (4.6 M). After 24 h modified materials were ready to use. The presence of poly(acrylic acid) onto the tested materials was confirmed by SEM (a JSM-5800 LV, JEOL device working at 25 kV) and XPS spectra obtained using a SPES ESCA system equipped with a Phoibos 100 analyser and SpecLab software. Electrolytic resistances (area resistance) of the modified PP membranes were $45 \pm 5 \text{ m}\Omega \text{ cm}^2$; before plasma treatment $120 \Omega \text{ cm}^2$. AC samples after plasma modification followed by induced graft polymerization of acrylic acid under UV irradiation, depending on procedure parameters, exhibited a grafting degree of poly(acrylic acid) onto AC electrodes expressed in wt% of 0.9 (AC1), 2.1 (AC2), 4.2 (AC3) and 9.7 (AC4); obtained data were taken as the average from 3 to 5 independent experiments.

2.4. Ionic conductivity of PP membrane

The experimental cell (Fig. 1) used to measure ionic conductivity of the membrane (electrolytic resistance) was composed of two compartments. Each one had two openings—one for a platinum electrode and one for a Hg/HgO reference electrode. These two compartments were fitted with water-tight gaskets. Determination of the electrolytic resistance of the membrane was performed by measurement of the potential between two reference electrodes at a fixed current I that flowed between platinum electrodes.

The electrolytic resistance (area resistance) of the membrane was determined by two successive measurements of potential difference between the reference electrodes; the first one without membrane (denoted as E), and the second one with the membrane (E'). In all measurements saturated LiOH solution (4.6 M) was used. The electrolytic area resistance R of the membrane was determined from the following equation [21]:

$$R = \frac{(E' - E)S}{I}$$

where S is the membrane surface area exposed to the electric field (7 cm^2), R is usually expressed in $\text{m}\Omega \text{ cm}^2$. Each measurement was made in 15 s after switching on the external circuit with fixed current I .

2.5. Contact angle measurements

Pieces of porous PP membranes were put into a laboratory press (190°C , 50 kG, 2 min) to get nonporous samples of this same material. Each sample was modified in the same way as the porous sample. Static contact angles of water and diiodomethane were measured by means of a Technicom TM 50 System equipped with a Panasonic GL 350 camera. At least 20 readings were made on each film. The surface tension and its polar and dispersive components were calculated according to harmonic averaging [22]. The polar and dispersive components of surface tension for testing liquids were taken according to Kuznietsov et al. [23]. Sample polarity was defined as a percent ratio of the polar component of surface tension and total surface tension.

2.6. Electrochemical measurements

After assembling the capacitor by contacting three “foils” (two modified AC electrodes separated by the modified PP membrane, all filled with saturated aqueous lithium electrolyte), and placing it

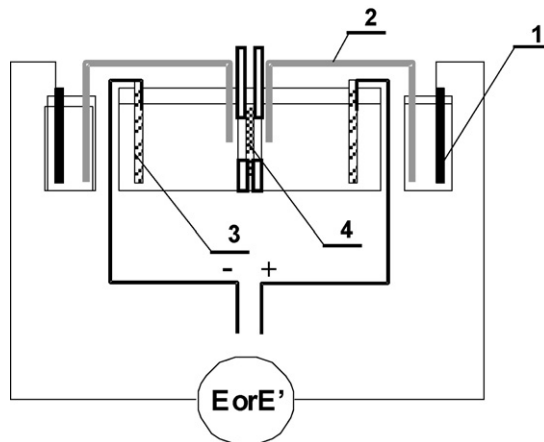


Fig. 1. Schematic representation of the experimental cell used to measure electrolytic area resistance of the membranes; 1—reference electrodes Hg/HgO; 2—salt-bridges; 3—Pt-electrodes; 4—membrane.

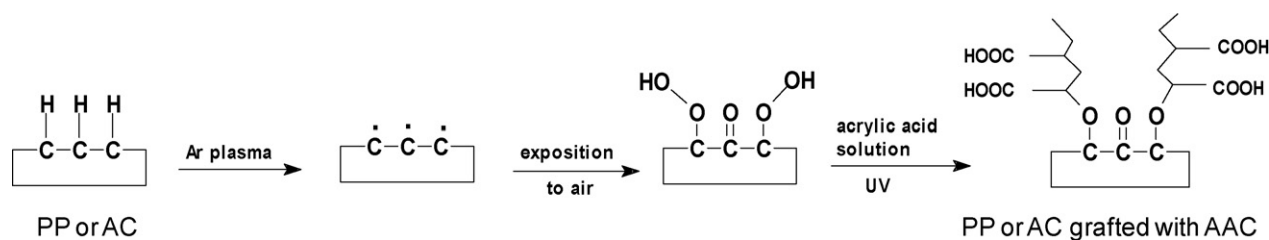


Fig. 2. The scheme of plasma-initiated grafting of acrylic acid onto PP or AC samples.

into the test vessel (Swagelok® system with stainless steel collectors) it was left at a temperature of *ca.* 50 °C in order to reach the equilibrium between the electrodes and the electrolyte. The final thickness of the tested capacitor was *ca.* 0.8 mm. The performances of the capacitors were characterized using cyclic voltammetry (CV), the galvanostatic charge–discharge test and electrochemical impedance spectroscopy (EIS). CVs (scan rate 10 mV s⁻¹) were performed using a potentiostat/galvanostat (μ AutoLab FRA2 type III, EcoChemie, Netherlands). The charge–discharge characteristics were carried out using the Atlas0461 MBI multichannel electrochemical system (Atlas-Solich, Poland). EIS measurements, over the frequency range from 0.001 Hz to 99 kHz and the potential amplitude of 10 mV, were performed using the μ AutoLab FRA2 type III electrochemical system (EcoChemie, Netherlands). All tests were conducted under ambient conditions.

3. Results and discussion

The main goal of the present study was permanent hydrophilization of hydrophobic PP and AC objects, by argon plasma treatment followed by graft polymerization of acrylic acid under UV irradiation, to make them usable as separator and electrode materials for EDLC devices.

Plasma treatment is known as a modern, clean, environmentally friendly and very efficacious modification technique of many surfaces. There are several ways of using plasma to change surface characteristics: plasma polymerization, plasma modification and plasma-initiated grafting. We applied the third technique and decided to use acrylic acid as a grafting monomer, for it is a low-boiling, water soluble, very reactive compound, which provides the surface with many hydrophilic carboxylic groups; modification of the surface by plasma only of such gases as argon or nitrogen increases the surface tension rapidly but the attained results diminish or even disappear with time.

Argon plasma is known to introduce on the surface a lot of radicals that are rapidly modified by contact with air into various functional groups, among others also peroxides and hydroxyperoxides. These, decomposed by UV light in the monomer solution, initiate its polymerization and hence create grafting chains on the material surface. The schematic path of the sample modification process is shown in Fig. 2. Moreover, Fig. 3 presents, as an example, representative SEM pictures of the cross-sections of PP and AC samples before and after plasma-grafting treatment and Figs. 4 and 5 show the XPS spectra of unmodified and modified PP and AC tested material, respectively.

3.1. Modification of PP samples

To achieve the assumed goal – an efficient separator for alkaline EDLC – one needs to choose the proper material. Microporous polypropylene membrane (Celgard 2500) seemed to be an excellent choice, from the above points. Its surface however is very hydrophobic (surface tension equal to 29.3 mN m⁻¹ with the polar component only 0.6 mN m⁻¹), so durable hydrophilization is nec-

essary to improve the wettability and hence electrolyte absorption and electrolytic conductivity. The electrolytic area resistance of a modified sample of PP membrane was taken as the first test of utility of the material obtained as a EDLC separator. The area resistance of unmodified membrane is equal to 120,000 m Ω cm².

Table 1 presents the values of contact angles of water and diiodomethane, and calculated from them, the values of surface tension and polarity for PP, sample after plasma treatment (PP-plasma), and sample after plasma treatment and AAC grafting in solution under UV irradiation (PP-modified). It contains also the electrolytic area resistance of the membranes examined.

Argon plasma treatment caused a very high increase of surface tension and polarity—the polar component became almost equal to the dispersive one, hence the polarity reached about 50%; unfortunately, electrolytic area resistance is still too high. After grafting, however, though it was done with polar monomer, one observes a decrease of polarity. Values of both surface tension and polarity stayed much higher than for polypropylene. These values are in good agreement with literature data; the author of work [24] has noted the surface tension of 35–39 mN m⁻¹ for polypropylene totally covered with grafted poly(acrylic acid).

The best results were obtained using plasma treatment membranes and grafting of acrylic acid in solution under UV irradiation (PP-modified); this case refers to the two step mechanism: plasma activation and grafting in solution. Effectiveness of this modification manner was confirmed by XPS technique (Fig. 4). This spectrum shows the presence of only carbon as observed at 284.6 eV, corresponding to C_{1s} core level (PP sample) and intense and narrow signal at 532.6 eV, corresponding to O_{1s} core level absent in virgin PP. XPS spectra of C_{1s} core level for the PP-modified sample (Fig. 4d) can be decomposed into two contributions appearing at 284.6 and 289.1 eV. These observed peaks were assigned to C–C, and –COO groups formed on the surface of tested sample.

3.2. Modification of AC samples

The untreated carbon fiber cloth was originally hydrophobic and repelled a drop of water. However, after plasma-grafting treatment its character changed. The drop of water put on the modified surface changed their volume very slowly at the beginning and disappeared completely after *ca.* 3 s. This qualitative observation shows on hydrophilization process of AC owing to introduction of some polar groups onto its surface by the procedure in question.

XPS observation was undertaken to analyze the functional groups formed by the plasma-grafting processing. XPS spectra of the AC sample are shown in Fig. 5. This spectrum (Fig. 5a) exhibited the presence of only carbon as observed at 284.6 eV, corresponding to C_{1s} core level. However, the AC-modified sample exhibited intense and narrow peak at 532.6 eV, corresponding to O_{1s} core level, as well as C_{1s} core level, as shown in Fig. 5b. As shown in Fig. 5c, XPS spectra of C_{1s} core level for the AC-modified sample can be decomposed into four contributions appearing at 284.6, 286.0, 287.5, and 289.1 eV. These observed peaks were assigned to C–C, C–O, C=O, and –COO groups formed on the surface of AC. This result

Table 1
Values of contact angle, surface tension and polarity of the samples chosen.

Sample's symbol	Contact angle [°]		Surface tension [mN m ⁻¹]	Polarity [%]	Electrolytic area resistance [mΩ cm ²]
	Water	CH ₂ I ₂			
PP	99.4	58.5	29.3	2.0	120,000
PP-plasma	44.5	41.7	56.5	46.7	112,000
PP-modified	82.9	53.7	38.5	20.1	40–50

demonstrates that poly(acrylic acid) was effectively induced onto the surface of the virgin AC sample via plasma-grafting treatment.

3.3. Electrochemical performance of EDLC with modified components

In order to examine the effect of plasma treatment on the performance of capacitors with modified components, model two-electrode capacitors were produced and CV tests of the capacitors were carried out. Fig. 6 shows specific capacitances of the capacitor modified electrodes, calculated from CV measurements, as a function of grafting degree of poly(acrylic acid) onto AC electrodes (AC1–AC4); a dashed line denotes capacitance of the capacitor with AC electrodes modified by HNO₃/H₂SO₄ mixture, and dotted one denotes capacitance of the capacitor with virgin AC electrodes, according to Ref. [25]. The electrolyte was 4.6 M aqueous LiOH solution in each test, and the scan rate and operating voltage were 10 mV s⁻¹ and 1.2 V, respectively. Specific capacitance trends was found to increase with the grafting degree, but the capacitance of modified AC samples for 9.7% of poly(AAc) decreased slightly from that of 4.2%, showing not a linear shape, but a volcano curve. Thus a working hypothesis may be proposed that excessive grafting causes a less usable surface area for the formation of the electric double layer and a higher resistance to the transport of electrolyte ions within micro-, meso and macro-pores of the AC electrode. Consequently, in our study it is considered that the “cold plasma” grafting of poly(AAc) onto AC in the range of ca. 4–9% (AC3 and AC4) is the best option for enhancing the performance of tested EDLCs, showing about two times larger specific capacitance (ca. 110 F g⁻¹) than e.g. an electrochemical capacitor with multi-walled carbon nanotubes as electrode materials modified by oxidation with an extremely oxidizing agent, such as mixed acid H₂SO₄/HNO₃ (51 F g⁻¹) in 1 M H₂SO₄ aqueous electrolyte, according to Ref. [25].

A detailed analysis of the electrochemical measurements characterized the performance of the tested capacitors with plasma modified separators and AC electrode materials (AC3 and AC4) has been performed using cyclic voltammetry (CV), the galvanostatic charge–discharge test and electrochemical impedance spectroscopy (EIS). Fig. 7a shows CVs for tested EDLCs at a scan rate of 10 mV s⁻¹. The CV profiles were nearly rectangular in shape (without visible peaks due to redox reactions), suggesting good capacitive devices in both cases. Moreover, good electric contacts at the electrode/electrolyte interface and good compatibility of all constituents of the unit capacitor are responsible for the good electrochemical characteristics. From the voltammograms, specific capacitances of the AC3 and AC4 electrodes were evaluated to be 114 and 103 F g⁻¹, respectively.

Galvanostatic charge–discharge curves for the experimental EDLC cells are shown in Fig. 7b. Linear curves were observed in each case. This type of capacitive behavior, with the square shape of voltammograms, confirms good synergy between all phases in the cell. Cell capacitance is deduced from the slope of the discharge curve with:

$$C = \frac{I}{dV/dt}$$

where C is cell capacitance in farads (F), I the discharge current in amperes (A) and dV/dt the slope of the discharge curve in volts per second (V s⁻¹). In a symmetrical system, where the active material weight is the same for the two electrodes, the specific capacitance C_{spec} in farads per gram of active material (F g⁻¹) is related to the capacitance of the cell C by:

$$C_{\text{spec}} = \frac{2C}{m_{\text{el}}}$$

where m_{el} is the weight (g) of the active material per electrode.

From the galvanostatic charge–discharge curves, at a current load of ±5 mA, specific capacitances of the electrodes, AC3 and AC4, were evaluated to be 119 and 110 F g⁻¹, respectively, and they are very close to those based on the CVs.

EIS, as a powerful technique for the investigation of the capacitive behavior of electrochemical cells, has also been used to verify the ability of the novel design of EDLC to store electrical energy. An example of Nyquist plots for the tested capacitors (both with plasma modified electrodes and a separator) are shown in Fig. 8a. In the high-frequency region of each spectrum there appears a single semicircle. From the point of intersecting with the real axis in the range of high frequency, resistance of the cell was estimated to be 2.35 Ω for the AC3 electrodes under this experimental condition, which is a little bit lower to that for the AC4 electrodes, i.e. 2.75 Ω. Following the semicircle with the decreasing frequency, the plots are transformed to a vertical line. A line close to 90° attributed to a capacitive behavior was observed for both cases; at higher frequencies, the capacitor behaves like a pure resistor and at low frequencies it shows capacitive behavior [26]. The specific capacitances of tested devices calculated from the imaginary part of the complex impedance spectrum: $C = (2\pi fZ'')^{-1}$ and plotted as functions of frequency are shown in Fig. 8b; obtained values are almost the same as those calculated from CVs and the charge–discharge test, i.e. 95 and 90 F g⁻¹. The capacitance is high at low frequencies for both cases and it starts to decrease at higher frequencies around 0.1–10 Hz. This region corresponds to the transition between the semicircle and the straight line in Fig. 8a.

Fig. 9a and b presents a simple way to model the capacitor frequency behavior by using impedance data, by analogy with the study published earlier [27,28]; this model shows relationships between $C'(\omega)$ – the real part of the capacitance $C(\omega)$ with $Z''(\omega)$ and $C''(\omega)$ – the imaginary part of the capacitance $C(\omega)$ with $Z'(\omega)$:

$$C'(\omega) = \frac{-Z''(\omega)}{(w|Z(\omega)|)^2}$$

$$C''(\omega) = \frac{Z'(\omega)}{(w|Z(\omega)|)^2}$$

$C'(\omega)$ corresponds to the capacitance of the cell that is measured during constant current discharge (direct current), and C'' corresponds to losses in the form of energy dissipation.

These figures present the variation of the real and the imaginary part of the capacitance with the frequency for the capacitors based on AC3 and AC4 electrodes. Fig. 9a shows the relationship between C' and frequency. At a low frequency (1 mHz), the capacitance of the electrode reached 0.47 F for the device with AC3 electrodes and 0.45 F for AC4 electrodes. This low frequency capacitance (C_{LF}) corresponds to the cell capacitance measured during galvanos-

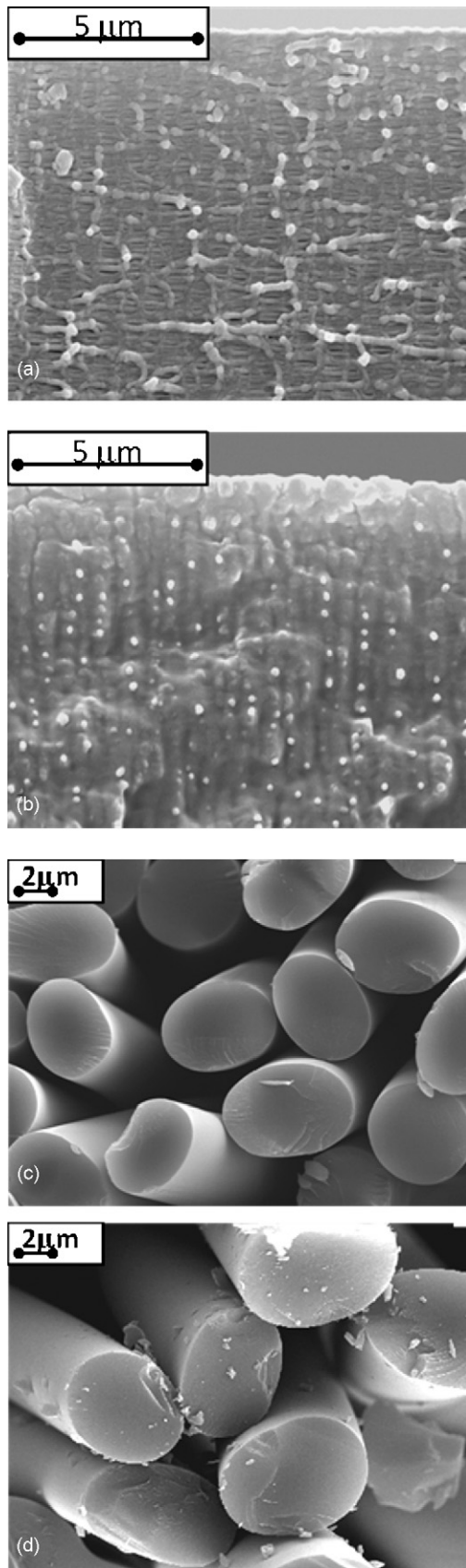


Fig. 3. SEM of cross-sections of PP (a and b) and AC (c and d) samples before (a and c) and after (b and d) plasma-grafting treatment.

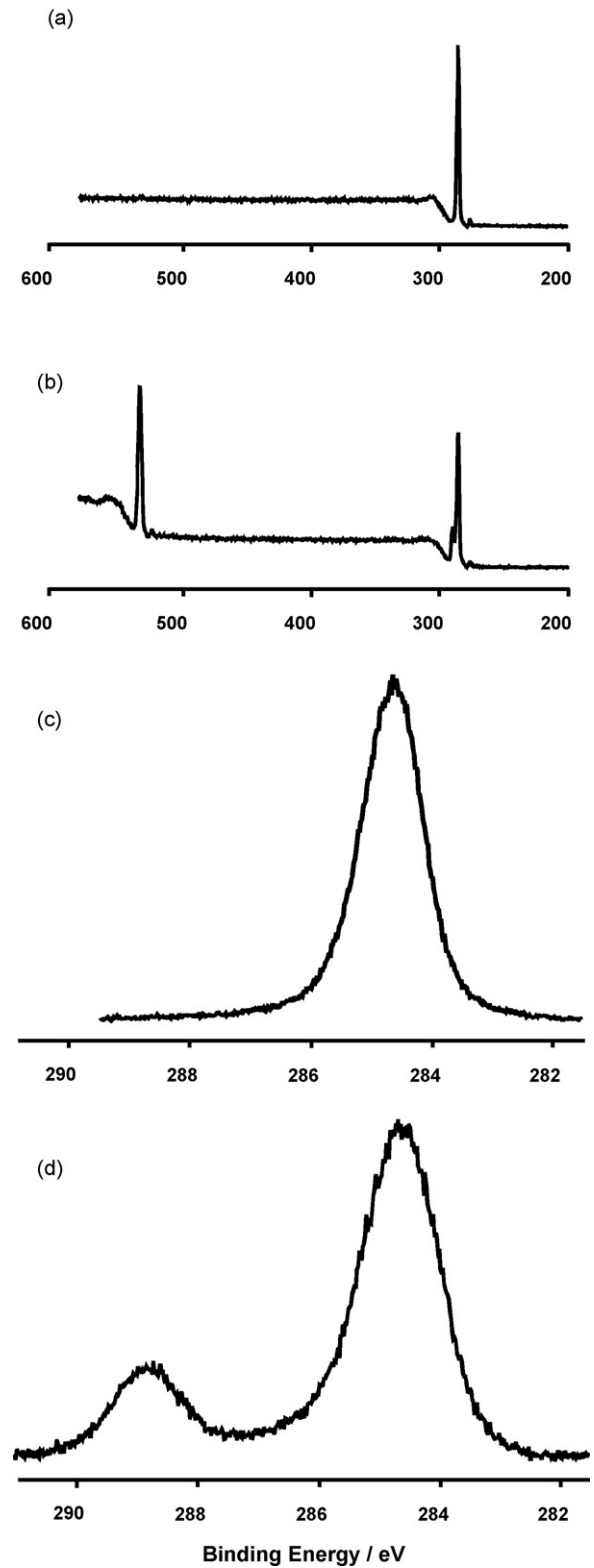


Fig. 4. XPS spectra of (a) virgin PP and (b) plasma-grafting modified PP membrane, (c) high resolution spectra of C_{1s} core level for virgin PP and (d) plasma-grafting modified PP membranes.

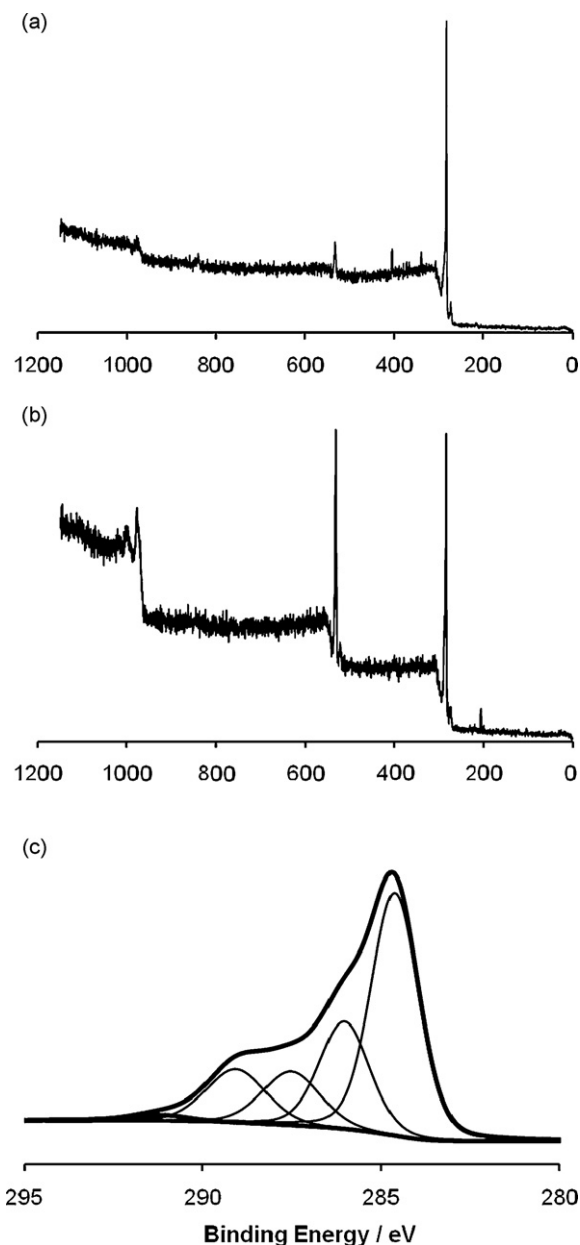


Fig. 5. XPS spectra of (a) virgin AC, (b) plasma-grafting modified AC and (c) high resolution spectra of C_{1s} core level for plasma-grafting modified AC (AC3 sample).

tatic cycling at ± 5 mA. When frequency is increased, capacitance decreases, and at a high frequency the capacitor behaves like a pure resistor. Fig. 9b shows the relationship between C'' and the frequency for the tested devices; C'' passes through a maximum at 52 mHz for the first case and 31 mHz for the second one. From this figure, it is possible to deduce the relaxation time constant that defines the frontier between the capacitive behavior and the resistive behavior of the capacitor. The relaxation time is deduced from the frequency f_0 with $\tau_0 = 1/f_0$; f_0 may be obtained from the real capacitance plot at $C' = C_{LF}/2$ and from the imaginary capacitance plot, where it corresponds to peak frequency.

The time constants are very different, as can be seen in Fig. 9b: 19.0 and 32.3 s, respectively, when using AC3 and AC4 electrodes (EDLCs with AC1 and AC2 electrodes: 42.2 and 38.3 s, respectively). The capacitor using AC3 electrodes is able to deliver its stored energy faster than the capacitor with AC4 electrodes, i.e. at a higher power. This is probably linked to the difference in the wettability between the two-electrode materials, leading to a difference

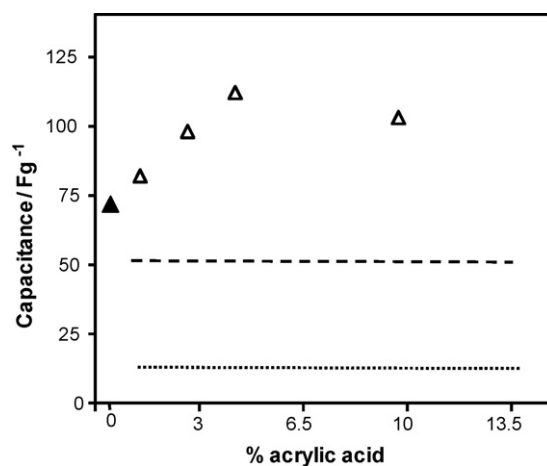


Fig. 6. Specific capacitances of plasma initiating grafting modified AC electrodes as a function of grafting degree of poly(acrylic acid). Data obtained from CVs measurements, scan rate 10 mV s⁻¹; (\blacktriangle) specific capacitance of AC electrodes after plasma treatment step only, dashed line denotes capacitance of capacitor with AC electrodes modified by HNO₃/H₂SO₄ mixture and a dotted one denotes capacitance of the capacitor with virgin electrodes, according to Ref. [25].

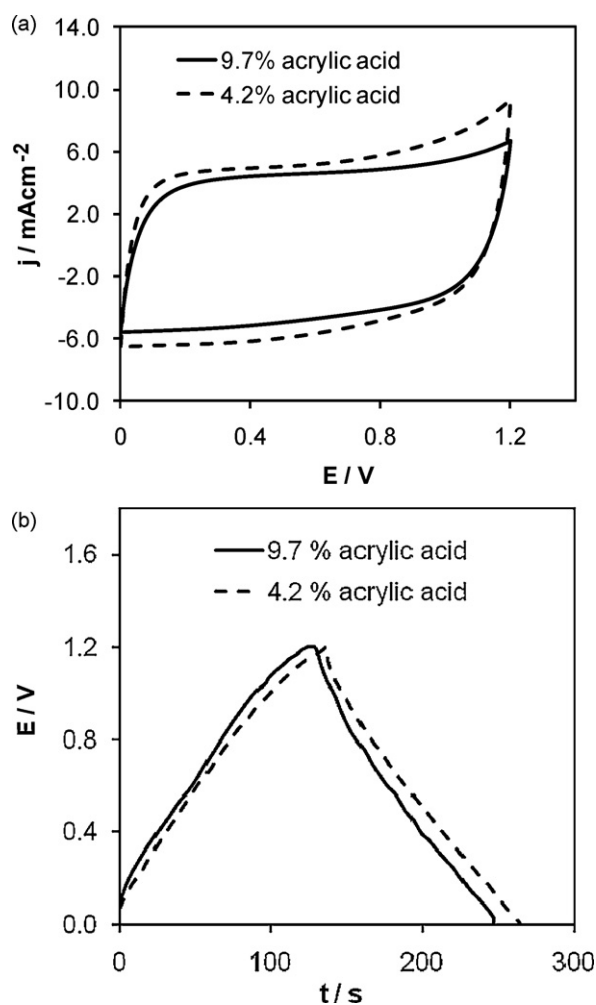


Fig. 7. (a) Cyclic voltammograms for plasma modified AC electrodes of EDLC cells with 4.6 M LiOH aqueous electrolyte. Scan rate 10 mV s⁻¹. (b) Charge-discharge curves (10th cycle) for EDLC with plasma modified AC electrodes with 4.6 M LiOH aqueous electrolyte. Charge-discharge current density ± 5 mA cm⁻².

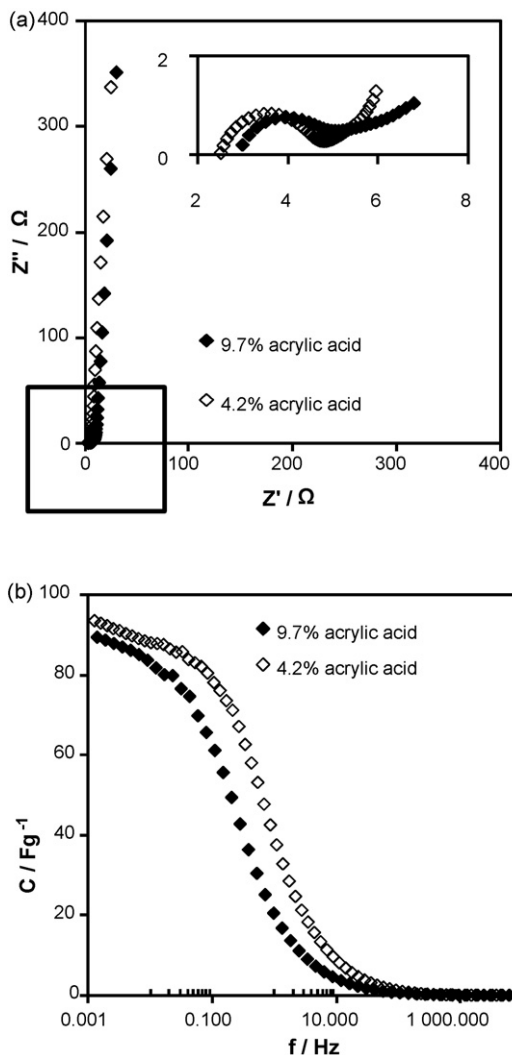


Fig. 8. (a) Nyquist plots for plasma modified AC electrodes of EDLC cells using 4.6 M LiOH aqueous electrolyte. (b) Capacitance vs. frequency plot obtained from EIS for tested EDLCs at 0 V applied potential.

in the electrolyte penetration inside the porous structure of the electrode material; the second reason is probably the blocking of AC surface by the excess of modifying poly(AAc). Best results are then obtained with plasma modified AC electrodes characterized by a 4.2% grafting degree of poly(AAc) onto/within the electrode material (AC3).

The stability of the prepared capacitor can be examined by conducting repeated charge–discharge cycling. A capacitor equipped with AC3 electrodes was charged and discharged between 0 and 1.2 V at 5 mA to confirm the stability. The coulombic efficiency of an electric double layer capacitor can be calculated from the equation [29]:

$$\eta = \left(\frac{t_d}{t_c} \right) \times 100$$

where t_d and t_c are the times required for discharge and charge, respectively. The variations of discharge capacitance and coulombic efficiency with cycle number are shown in Fig. 10. The results show that the capacitor has a stable capacitance (about 105 Fg⁻¹) and coulombic efficiency (about 98%) over 1000 cycles; only 10% of the initial capacitance is lost after 6000 cycles, indicating that the capacitor has a good cycle life.

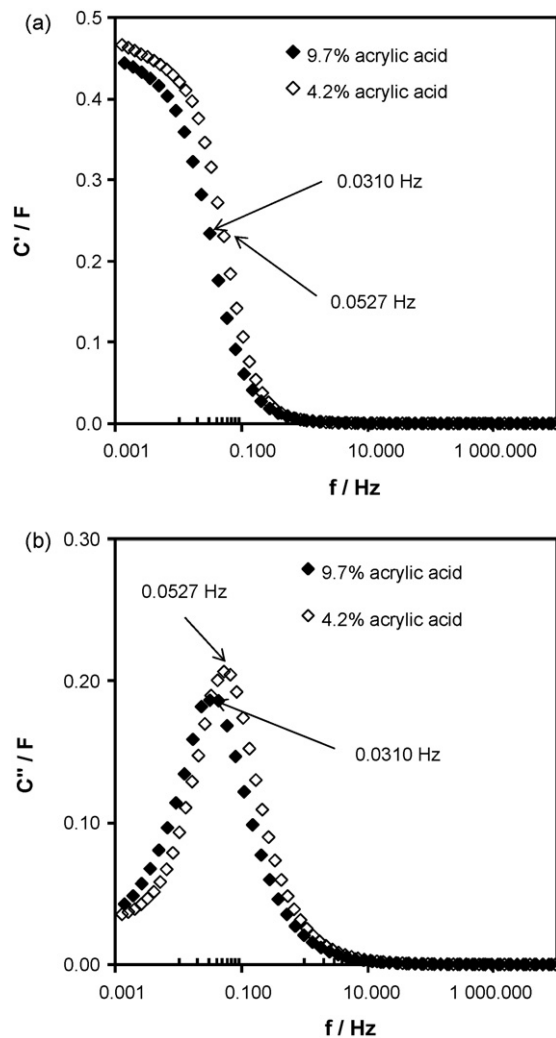


Fig. 9. (a) Evolution of the real part of capacitance vs. frequency for tested cells. (b) Evolution of the imaginary part of capacitance vs. frequency for tested cells.

Rate capabilities of the cells with AC3 electrodes were also examined at various current rates. Fig. 11 shows the Ragone chart with the plots calculated from the discharge data of the galvanostatic charge/discharge curves measured at constant current densities of 0.1, 0.5, 1.0, 1.5, 2.0, 5.0 and 10 A g⁻¹; the energy density of the cell was calculated by using the total weight of the active

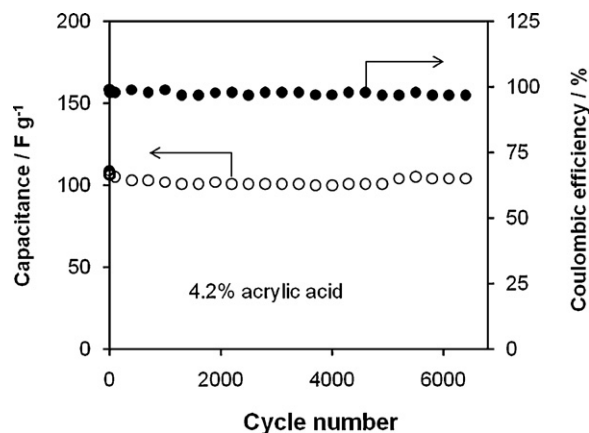


Fig. 10. Variation of specific capacitance stability and coulombic efficiency with cycle number for tested EDLC charges and discharged at 5 mA in 4.6 M LiOH solution.

Table 2
Characteristics of tested EDLCs.

EDLCs	C_{\max} [$F g^{-1}$]	E_{\max} [$kJ kg^{-1}$]	P_{\max} [$kW kg^{-1}$]
ACs ^a (4.7 M LiOH)	114 ^b , 119 ^c , 95 ^d	32.3	14.4
ACFC ^e (0.8 M TEABF ₄ in PC)	20 ^c	–	–
ACFC ^f modified 'cold' plasma (0.8 M TEABF ₄ in PC)	23 ^c	–	–
AC ^f (0.1 M H ₂ SO ₄)	29 ^b	–	–
AC ^f -modified RF plasma (0.1 M H ₂ SO ₄)	38.9 ^b	–	–
ACFs ^g (0.5 M H ₂ SO ₄)	111 ^b	–	–
ACFs ^g modified RF plasma (0.5 M H ₂ SO ₄)	142 ^b	–	–
CNs ^h (0.1 M H ₂ SO ₄)	44 ^b	–	–
CNs ^h immersed in 15 wt.% HNO ₃ (0.1 M H ₂ SO ₄)	110 ^b	–	–
CNs ^h modified RF plasma (0.1 M H ₂ SO ₄)	128 ^b	–	–

C_{\max} —specific capacitance; E_{\max} —maximum energy stored; P_{\max} —maximum power.

^a This study.

^b Calculated from CV measurements.

^c Calculated from galvanostatic measurements.

^d Calculated from EIS measurements.

^e ACFC—activated carbon fiber cloth [14].

^f AC—activated carbon [18].

^g ACFs—activated carbon fibers [30].

^h CNs—carbon nanotubes [17].

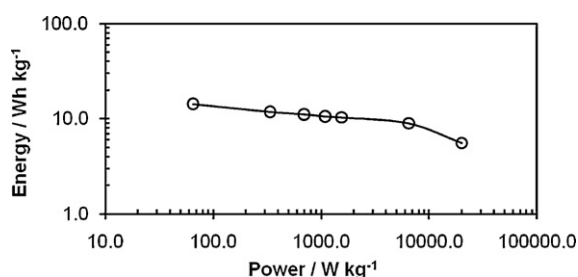


Fig. 11. The Ragone plot for a capacitor with plasma modified AC (AC3 sample) and PP components in 4.6 M LiOH solution. Data obtained from galvanostatic charge–discharge cycling with current densities varying from 0.1 A g⁻¹ to 10 A g⁻¹.

electrode materials, the cell voltage and the capacity based on the galvanostatic discharge curve. The data in Fig. 11 clearly demonstrated that the tested device has a good specific energy and power density. For example, the specific energy was 12 Wh kg⁻¹ at a power density of 330 W kg⁻¹, and it still maintains 9 Wh kg⁻¹ at a power density of 6 kW kg⁻¹; it is comparable with commercialized EDLCs and can be competitive with acid or alkaline batteries, but with a higher power density, long cycling life, and using low cost, environmentally friendly materials.

The electrochemical properties of tested devices calculated from cyclic voltammetry, galvanostatic charging–discharging and impedance spectroscopy are shown in Table 2; it also contains literature data of available similar devices. Presented data provide valuable information for the development of novel compositions of EDLCs with a “cold plasma” modified electrode and separator materials in aqueous LiOH electrolyte.

4. Conclusion

In conclusion, the electrochemical performance of coin cell capacitors assembled with AC fiber cloth electrodes and PP separator, both modified by plasma treatment with subsequent grafting with acrylic acid under UV irradiation, using 4.6 M LiOH electrolyte was systematically studied. The results obtained are summarized as follows: The AC and PP surface was changed from hydrophobic to hydrophilic and the presence of poly(acrylic acid) on these specimens was confirmed by XPS. The capacitors prepared in the present work exhibit excellent capacitance stability with a coulombic efficiency of 98% over 1000 cycles. At the 1000th cycle of potential cycling (1 A g⁻¹) the specific capacitance of 110 F g⁻¹ was obtained with a specific energy of 11 Wh kg⁻¹ at power density of 1 kW kg⁻¹.

The above results provide valuable information which may be used when developing novel compositions of EDLCs.

Acknowledgment

This study was financially supported by the Poznan University of Technology (BW 31-206/2010).

References

- [1] B.E. Conway, *Electrochemical Supercapacitors—Scientific Fundamentals and Technological Applications*, Kluwer Academic/Plenum Publishers, New York, 1999.
- [2] O. Hass, E.J. Cairns, *Annu. Rep. Prog. Chem., Sect. C* 95 (1995) 163–197.
- [3] R. Kotz, M. Carlen, *Electrochim. Acta* 45 (2000) 2483–2498.
- [4] E. Frackowiak, F. Beguin, *Carbon* 39 (2001) 937–950.
- [5] H.P. Boehm, *Carbon* 32 (1994) 759–769.
- [6] T. Momma, X. Liu, T. Osaka, Y. Ushio, Y. Sawada, *J. Power Sources* 60 (1996) 249–253.
- [7] S. Biniak, B. Dzielendziak, B. Siedlewski, *Carbon* 33 (1995) 1255–1263.
- [8] K. Kierzek, E. Frackowiak, G. Lota, G. Gryglewicz, J. Machnikowski, *Electrochim. Acta* 49 (2004) 515–523.
- [9] K. Babel, K. Jurewicz, *J. Phys. Chem. Solids* 65 (2004) 275–280.
- [10] B. Xu, F. Wu, R. Chen, G. Chen, G. Cao, S. Chen, Z. Zhou, Y. Yang, *Electrochem. Commun.* 10 (2008) 795–797.
- [11] K. Hyeok An, K.K. Jeon, J.K. Heo, S.C. Lim, D.J. Bac, *J. Electrochem. Soc.* 149 (2002) A1058–A1062.
- [12] K. Jurewicz, S. Depleux, V. Bertagna, F. Beguin, E. Frackowiak, *Chem. Phys. Lett.* 347 (2001) 36–40.
- [13] M. Ishifune, R. Suzuki, Y. Mima, K. Uchida, N. Yamashita, S. Kashimura, *Electrochim. Acta* 51 (2005) 14–22.
- [14] M. Ishikawa, A. Sakamoto, M. Merita, Y. Matsuda, K. Ishida, *J. Power Sources* 60 (1996) 233–238.
- [15] X. Li, K. Horita, *Carbon* 38 (2000) 133–138.
- [16] L.E. Cascarini De Tora, E.J. Bottani, A. Martinez-Alonso, A. Cuesta, A.B. Garcia, J.M.D. Tascon, *Carbon* 36 (1998) 277–282.
- [17] C.C. Li, H.C. Huang, *J. Power Sources* 188 (2009) 332–337.
- [18] C.C. Li, C.C. Yen, *J. Appl. Electrochem.* 37 (2007) 813–817.
- [19] A. Ciszewski, I. Gancarz, J. Kunicki, M. Bryjak, *Surf. Coat. Technol.* 201 (2006) 3676–3684.
- [20] A. Ciszewski, J. Kunicki, I. Gancarz, *Electrochim. Acta* 52 (2007) 5207–5212.
- [21] S.U. Falk, A.J. Salkind, *Alkaline Storage Batteries*, John Wiley & Sons, Inc., New York, 1969, p. 240.
- [22] S. Wu, *Polymer Interface and Adhesion*, Dekker, New York, 1982.
- [23] A.Y. Kuznetsov, V.A. Bagrgansky, A.K. Popov, *J. Appl. Polym. Sci.* 47 (1993) 1175–1184.
- [24] F. Poncin-Epaillard, B. Chevet, J.C. Brosse, *J. Appl. Polym. Sci.* 53 (1994) 1291–1306.
- [25] Y.-T. Kim, T. Mitani, *J. Power Sources* 158 (2006) 1517–1522.
- [26] R. De Levie, *Electrochim. Acta* 8 (1963) 751–780.
- [27] C. Portet, P.L. Taberna, P. Simon, C. Albery-Robert, *Electrochim. Acta* 49 (2004) 905–912.
- [28] C. Portet, P.L. Taberna, P. Simon, E. Flahaut, *J. Power Sources* 91 (2005) 371–378.
- [29] T. Osaka, X. Liu, M. Nojima, T. Momma, *J. Electrochem. Soc.* 146 (1999) 1724–1729.
- [30] K. Okajima, K. Ohta, M. Sudoh, *Electrochim. Acta* 50 (2005) 2227–2231.